

Chapter 9

Discussion and conclusions

Data analyzed in this study were recorded within altogether five campaigns carried out in two study areas. The electromagnetic image of the continental margin of the Southern Andes at latitude $\sim 39^\circ\text{S}$ turned out to be very different from that of the Central Andes around latitude $\sim 21^\circ\text{S}$. Whereas various strong conductivity anomalies are encountered to the north, absolute values of conductivities in the south are comparably small. Yet, there is strong evidence for electrical anisotropy in the southern study area.

In addition to the regional investigations, this study has also a clear methodological focus: to exploit the simultaneous nature of the array data by multivariate processing and inter-station transfer function analysis, which involves also an inversion of such data, what had first to be implemented. The rather different aspects of this study are discussed below.

Methodological Aspects

Multivariate processing

Sub-arrays consisting of 3–6 simultaneously running stations were formed, subjecting their data to a multivariate analysis that calculates a spectral density matrix (SDM), containing the array's inter-component cross- and power-spectra (*Egbert and Booker [1989], Egbert [1997]*, chapter 4). Generally the two eigenvectors belonging to the two largest eigenvalues of the SDM provide an estimate of the array's response space to approximately uniform sources, and further eigenvalues, if significantly above zero, represent coherent noise. From the response space, any possible inter-component transfer functions within the array can be calculated, including also local transfer functions that are usually calculated by bivariate analysis of local data, which involves data from a reference station only to account for locally coherent, but spatially incoherent noise in the input channels. It shall be mentioned here that inter-station transfer functions can certainly also be estimated by standard bivariate analysis techniques (e.g., *Schmucker [1970]*).

Noise which is coherent throughout the array, though observed in both, the northern and, stronger, the southern study area, turned out to be low enough that for local transfer functions, differences between the local bivariate analysis and the multivariate array analysis were minute in terms of both, the values and the quality of the transfer functions. Therefore, all local transfer functions analyzed in this work are taken from a local bivariate analysis, and multivariate analysis results were only used for the derivation of inter-station data.

Combination of the processed arrays

In the northern study area around $\sim 21^\circ\text{S}$, not all processed sub-arrays have a common reference, since the data originate from different campaigns. The internal structure of the data from the separate campaigns partly also does not allow to choose one common reference. However, as *almost* all processed arrays are somehow spatially overlapping, they can be successively combined to one final synthetic array, so that the fields of all stations can be related to an arbitrary common reference (section 4.3). Yet, since stations in Chile and Bolivia never ran simultaneously, this is not possible without making the assumption that the two stations closest to the political border have the same horizontal magnetic field, which cannot be valid in a strict sense. Therefore, data from this synthetic array were only used for illustration (chapter 5) and ‘qualitative’ modelling (*Soyer and Brasse [2001]*).

Discussion of the processed data

In both study areas, inter-station geomagnetic data are in high agreement with local geomagnetic and magnetotelluric data, pointing out again the consistency between results of both processing methods. The strong inductive effect of the Pacific ocean, which reaches depths of almost 8 km to the north and more than 4 km to the south, dominates the data far beyond the Longitudinal resp. Central Valley, and leads to a decrease of the horizontal field onshore with only slightest spatial gradients (chapter 5 and section 7.1). However, inter-station geomagnetic data (often also referred to as geomagnetic perturbation) close to the coast reflect enormous gradients of the horizontal magnetic variation field. This corresponds to the observation of anomalous impedance phases in this area, interpreted by *Lezaeta [2001]* as strong current channelling involving also magnetic effects. Geomagnetic perturbation data allow a more quantitative determination of the observed magnetic distortion effects, revealing that the observations fit the quasi-static distortion model, which formally describes the anomalous magnetic field as the result of a multiplication between a real, frequency-independent matrix and the regional undistorted electric field (equation 5.2). Due to the strong sea-land conductivity contrast, the regional impedances of the TM-polarization exceed those of the TE-polarization by several orders of magnitude. This manifests itself in the observation that only perturbation data related to an inducing magnetic field parallel to the coast line are affected by the distortion. The data needed for a two-dimensional analysis are nicely unaffected. The distortion analysis presented in section 5.1 seems to be extendable e.g., to the determination of the local distorter’s orientation, assuming an elongated geometry as in *Lezaeta [2001]*.

2-D inversion of inter-station geomagnetic transfer functions

To two-dimensionally analyze the in general rarely investigated inter-station geomagnetic data with up-to-date methods, a recently published 2-D inversion code for electromagnetic induction data (REBOCC, *Siripunvaraporn and Egbert [2000]*) was extended for inversion of the two non-zero elements of the geomagnetic perturbation matrix, the horizontal to horizontal transfer functions $B_y/B_{y0} - 1$ and the vertical to horizontal transfer functions B_z/B_{y0} (chapter 6). Most crucial implementations were associated with the essential calculation of sensitivities, the derivation of the responses with respect to the model parameters. This topic

has been approached straight forward, following *Rodi* [1976], as it has also been done in the calculation of the local responses' sensitivities. Starting from a recently derived uniqueness theorem on the 2-D conductivity structure explaining local geomagnetic transfer functions (induction vectors), also the general uniqueness of models explaining ideal inter-station 2-D data sets (continuous in time/frequency and space) could be deduced (section 6.1.2).

Synthetical examples

The new features have been tested by inversion of synthetic data of two very different models, forward calculated by the program of *Wannamaker et al.* [1987]. Convergence was good for both data types and models, demonstrating that the implementation was in principle successful.

The worthiness of an investigation of horizontal perturbation data, however, depends strongly on the geometry of subsurface conductivity anomalies. Above a series of deep-seated 2-D anomalies of small lateral extent, horizontal geomagnetic perturbations can resolve lateral boundaries of conductors significantly worse than transfer functions involving the vertical magnetic field component, since the latter undergoes changes of sign above the lateral contrasts, whereas the horizontal magnetic field might show only slight spatial variation around a rather constant level (section 6.4.1). In contrast, above laterally extended anomalies, where resolution of the locally 1-D conductivity distribution is aspired, the vertical magnetic field nearly vanishes, whereas the anomalous horizontal field, when related to a reference aside the anomaly, as a function of period bears information on the locally 1-D structure (section 6.4.2). Still, having ideal data that are continuous in space, the vertical magnetic field can be transformed into the horizontal field by applying a Hilbert transformation (section 6.1.2). The choice of a proper 'normal' reference station is less crucial for an inversion of perturbation data than for a forward modelling investigation, since the algorithm can also handle field anomalies induced by enhanced conductivities below the reference station, which would provide a difficult data set for the task of a forward modelling.

As a further extension, the possibility to invert data where the field of every station is related to that of an individual reference was implemented. Synthetic results obtained with such data were essentially worse: relating the horizontal fields of a station above the anomaly to that of another station above the same anomaly implies a significant loss of information compared to a data set where all fields are related to a common reference aside the anomaly (section 6.4.3).

Results of regional investigations

Processes taking place at an active continental margin are strongly suggested to significantly increase the electrical conductivity of materials in various regions of the subsurface. Therefore, electromagnetic methods can give insights in these processes by measuring the spatial distribution of this physical property. A very good conductor encountered in the study areas is the Pacific ocean, which is not a target of investigation. Unfortunately, its inductive effect is so strong, that postulated conductivity anomalies near the ocean provoked by water release due to compaction of subducted sediments and phase transitions in the subducted slab (*Peacock* [1996]) can hardly be resolved with electromagnetic measurements, the more so if only onshore magnetic data are analyzed (*Evans et al.* [2002]). This was realized in the

previous electromagnetic studies in the Central Andes and accordingly also in this study for both study areas, even though due to the sedimental fill of the trench, higher conductivities might be expected above the slab in south Chile (chapters 5, 7). Also, geometries within the accretionary complex of the leading edge of the South American continent cannot be imaged without offshore data.

Central Andes

Data quality of geomagnetic inter-station transfer functions calculated from the joint synthetic arrays was too bad, and their physical content too questionable for a full quantitative modelling. Therefore, geomagnetic perturbation data used in the inversion are mostly taken directly from the processed arrays, and are therefore not related to a common reference. Considerations on the invertability of such data as well as synthetic modelling results make clear that this is a significant drawback (section 6.4.3). At least for the Chilean part of the ANCORP profile, most data can be related to the common station CTE, located in the Longitudinal Valley.

Two zones of enhanced conductivity are observed in the forearc of the northern study area. The anomalies in the Coastal Cordillera manifest themselves mainly on account of their quasi-static effects, and the depth extent of these structures is difficult to resolve (section 5.1 and *Lezaeta* [2001]). Possible causes of the conductivity enhancement, e.g. saline fluids circulating within the Atacama fault system, are discussed in *Lezaeta* [2001]. The second zone of anomalous conductivity in the forearc is found below the Precordillera, with higher conductivities to the north (Pica profile). The effect of this zone is particularly strong in the magnetic field. Inversion of magnetic data from the ANCORP profile revealed that the magnetic variation anomaly can be explained by high conductivities below the surface (several kms). Inclusion of magnetotelluric data places the conductivity enhancement at greater depth, and joint inversion of local or inter-station tipper functions (T_y or z_D) together with impedance data of the TM-polarization, splits the anomaly into two parts, as it was also modelled by *Echternacht et al.* [1997] and *Lezaeta* [2001]. The downward extension of the lower anomaly, as well as conductivities just above the slab are difficult to resolve. As for the Coastal Cordillera, saline fluids are preferably discussed to account for the Precordillera anomaly (*Echternacht et al.* [1997], *Lezaeta* [2001]). Conductivities below the Western Cordillera (the active volcanic arc), are – if at all – only slightly enhanced and of three dimensional geometry, reflected in the anomalous impedance phases in the transverse polarization (figures 5.2, 7.4 top, and 7.5 bottom).

The Altiplano is characterized by very high conductivities close to the surface (sediments) and below ~ 20 km depth (“Altiplano Conductivity Anomaly”, *Schwalenberg* [2000], *Brasse et al.* [2002], and this study). As also observed in the western part of the profile, geomagnetic data of the different types (local: B_z/B_y , inter-station: B_y/B_y^0 and B_z/B_y^0) are highly consistent, which is reflected in the similar results of their separate inversions, and a good data fit in the joint geomagnetic inversions. Previous analysis of data from the Altiplano did not include any magnetic transfer functions and modelled an upwelling of the Altiplano conductor in the Central Altiplano. This is not consistent with geomagnetic data: To explain magnetic data on the Altiplano, strong anomalous currents and thus enhanced conductivities are required in the eastern part of the Altiplano. Still, it has to be pointed out that both, impedance and geomagnetic data have three-dimensional characteristics in this area.

From an analysis of geomagnetic variations, *Schmucker et al.* [1966] deduced the “Andean Conductivity Anomaly”, running north of this study area below the eastern part of the Altiplano and the Eastern Cordillera (3.4). *Krüger* [1994] and *Schwarz and Krüger* [1997], incorporating local tipper functions in a 2-D analysis of data from stations slightly south of 21°S, also modelled higher conductivities in the eastern Altiplano. Furthermore, seismic attenuation of L_g phases, as deduced by *Baumont et al.* [1999], has a maximum in the eastern part of the Altiplano just north of the study area. Due to the frequency-independence of this attenuation, *Baumont et al.* [1999] favor scattering causing the attenuation, and also with respect to the low Poisson number of ~ 0.25 derived by *Zandt et al.* [1996], exclude a percentage of partial melt $>1\%$. In contrast, *Schmitz et al.* [1997] and *Schilling and Partzsch* [2001] within multidisciplinary investigations by considering laboratory data, results from various seismic experiments, gravimetric data, conductivity anomalies and heat flow data, estimate a portion of partial melt of approx. 20 vol.% in the Andean crust below the Altiplano. Recent thermo-mechanical modelling studies suggest that only convective heat and mass transfer by partially molten lower crust material can account for the proposed partial melt ratios (*Babeyko et al.* [2002])

Considering the results from the synthetic modelling, the Altiplano conductor would be a good target for an analysis of horizontal inter-station transfer functions, if all data on top of this anomaly could directly be related to a reference aside of it. Modelling of such data could to a certain extent resolve the vertical conductivity distribution, which is not possible with the available inter-station data. A particularly favourable data set would be simultaneous across the whole mountain chain with common references on both sides of it.

Southern Andes

Electromagnetic conductivity in the southern study area has been modelled following two different approaches, depending on the transfer functions analyzed: i) isotropic 2-D inversion, since most data are clearly dominated by two-dimensional electrical structures of a structural strike corresponding with the morphological strike (section 7.4), and ii) anisotropic 2-D forward modelling of the geomagnetic north component of local induction vectors, since these are uniformly deviated towards north throughout the study area, without gradient along the structural strike direction, thus indicating a 2-D conductivity distribution with horizontal anisotropy of a strike differing from the structural strike (section 8). It has been illustrated that the enormous land–sea contrast is an ideal environment for the detection of such anisotropy by geomagnetic transfer functions.

Isotropic investigations revealed enhanced conductivities in 20–40 km depth below and east of the volcanic arc, which is supposed to be controlled by the Liquiñe-Ofqui fault. An anomaly in the Central Valley in the northern profile, two-dimensionally modelled in *Brasse and Soyer* [2001], was identified as three-dimensional, manifested in apparent resistivities and phases of the TE-polarization impedances mostly. Joint inversions of geomagnetic data revealed high consistency between the geomagnetic east and vertical components in terms of a 2-D current density geometry, which also has to be expected in 2-D anisotropic conductivity distributions. Anisotropic 2-D modelling aimed at finding simple conductivity distributions which can explain the geomagnetic north component of local induction vectors. These models contain

a horizontally anisotropic continental layer with an upper boundary in the mid crust, integrated conductivities of $\tau_{\parallel} \approx 800 \text{ S}$ and $\tau_{\perp} \lesssim \tau_{\parallel}/30$, and an anisotropy strike ranging between N25°E and N70°E. Electrical anisotropy within the subducted Nazca plate can not explain the observed data set.

Though the isotropic and the anisotropic models naturally disagree, they are suggested to reflect important aspects of the true conductivity distribution. The anisotropic continental layer is supposed to be linked with regional tectonics. The anomaly below the magmatic arc, modelled by isotropic inversion, is supposed to be linked with magmatism. But magmatism also is supposed to be linked with tectonics: *Namakura* [1977] proposed that the regional tectonic stress orientation can be taken from the spatial distribution of flank eruptions on the slope of composite volcanoes. These eruptions are regarded as surface features which indicate the pattern of radial dykes developing from the central conduit. In regimes with significant tectonic stress, these dykes are likely to develop perpendicular to the direction of minimum horizontal compression, i.e. parallel to the direction of maximum horizontal stress. As an example, *Namakura* [1977] presented schematic maps of 10 volcanoes and their parasitic vents from the Southern Andes between 37.5°S and 41.5°S, showing a clearly visible concentration of the sites of flank eruptions in a zone trending N55°–75°E (figure 9.1; in an extended investigation, *López-Escobar et al.* [1995] deduced a preferred orientation of N50°–70°E). This is also observed at the three volcanoes Villarrica, Quetrupillan and Lanin, which are themselves roughly aligned on the NW trending Gastre fault. Apart from such exceptions, also the alignment of many stratovolcanoes and minor eruptive centers follows this trend (*López-Escobar et al.* [1995]). Confirming the model of *Namakura* [1977], kinematic analysis of fault slip data indeed revealed a principal compressional stress orientation in NE-SW direction for Quaternary tectonic events within the intra-arc zone (*Lavenu and Cembrano* [1999]). By finite element modelling of the continental stress field north of the Chile triple junction (46°S), where the Chile Ridge is colliding with the South American continent, *Nelson et al.* [1994] demonstrated that the development of a northward moving forearc sliver west of the Liquiñe-Ofqui fault might be caused by a combination of both, an indenter effect due to the impingement of the Chile Rise, and the obliqueness of convergence, which is today $\sim 25^\circ$ with respect to the orthogonal. The orientation of the modelled stress field resulting from a combination of the two effects also fits well with the above observations.

It may be concluded that a significant part of the volcanism may be related to vertical feeder dykes. The basaltic to andesitic basaltic nature of volcanic rocks from Late Pleistocene to Holocene indicates a short residence time of the magmas in the crust and accordingly a rapid ascent of these (*López-Escobar et al.* [1995]). *Emerman and Marrett* [1990] pointed out that such low-viscous intrusions are presumably of sheet-like geometry at all depths within the lithosphere, their orientation reflecting the stress orientation at the respective depth.

Electromagnetic data suggest that the development of vertical dykes parallel to the maximum horizontal stress direction is not confined to a narrow band below the magmatic arc, but extends perpendicular to the structural strike in both directions. Still, molten material must be concentrated and (naturally) upwelled below the volcanic arc, as indicated by both, raw data and isotropic modelling results. Such imagination might be helpful in the development of a model, which is able to explain most part of the transfer functions obtained in this study area.

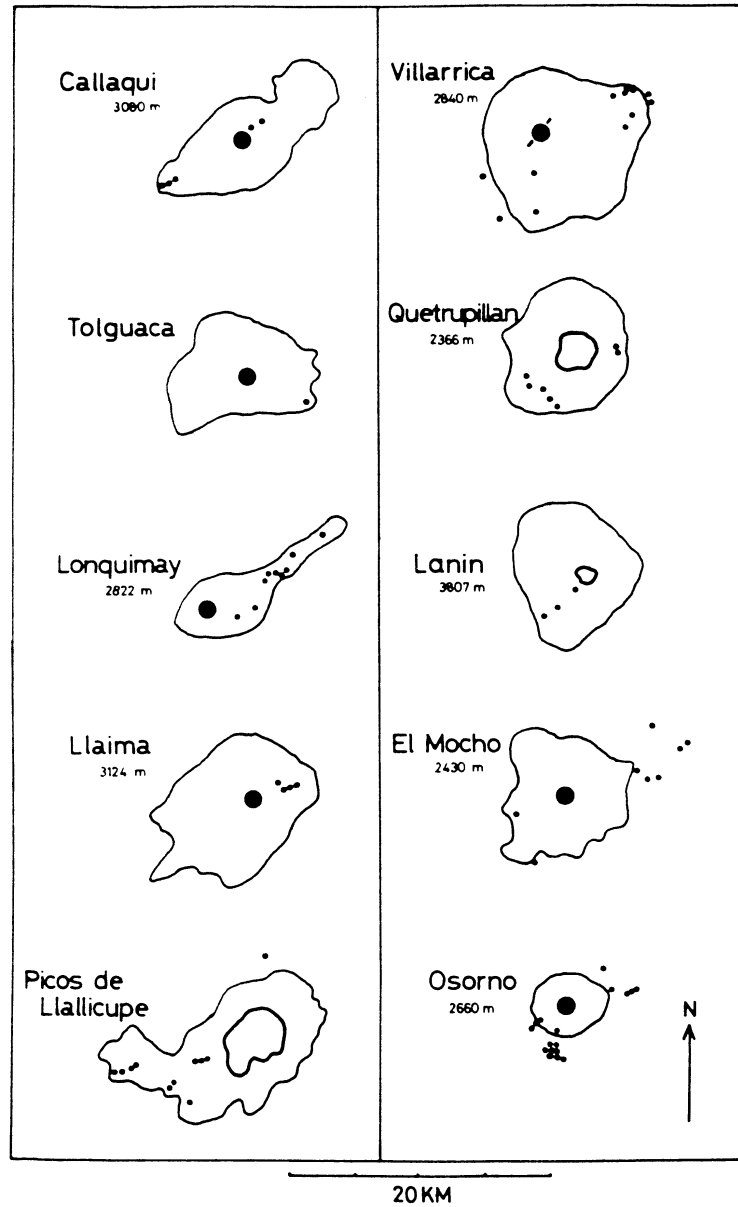


Figure 9.1: Distribution of flank crater eruptions of stratovolcanoes in the Southern Andes between 37.5°S and 41.5°S . Flank eruptions concentrate mostly in a zone trending $\text{N}55^{\circ}\text{--}75^{\circ}\text{E}$ (from Namakura [1977]).

